THE JOURNAL OF PHYSICAL CHEMISTRY Letters

Letter

pubs.acs.org/JPCL

Stacking Faults and Mechanical Behavior beyond the Elastic Limit of an Imidazole-Based Metal Organic Framework: ZIF-8

Vinay I. Hegde,[†] Jin-Chong Tan,[‡] Umesh V. Waghmare,*[,†] and Anthony K. Cheetham*[,¶]

[†]Theoretical Sciences Unit, Jawaharlal Nehru Centre for Advanced Scientific Research, Jakkur, Bangalore 560 064, India

[‡]Department of Engineering Science, University of Oxford, Parks Road, Oxford OX1 3PJ, United Kingdom

[¶]Department of Materials Science and Metallurgy, University of Cambridge, Pembroke Street, Cambridge CB2 3QZ, United Kingdom

ABSTRACT: We determine the nonlinear mechanical behavior of a prototypical zeolitic imidazolate framework (ZIF-8) along two modes of mechanical failure in response to tensile and shear forces using first-principles simulations. Our generalized stacking fault energy surface reveals an intrinsic stacking fault of surprisingly low energy comparable to that in copper, though the energy barrier associated with its formation is much higher. The lack of vibrational spectroscopic evidence for such faults in experiments can be explained with the structural instability of the barrier state to form a denser and disordered state of ZIF-8 seen in our analysis, that is, large shear leads to its amorphization rather than formation of faults.

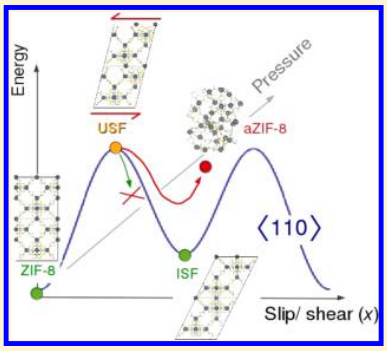

SECTION: Surfaces, Interfaces, Porous Materials, and Catalysis

Among metal−organic frameworks (MOFs) with a diverse range of structures, pore geometries, and chemical functionalities, the zeolitic imidazolate frameworks (ZIFs) combine the pore size tunability of MOFs and the thermal stability of zeolites, making them highly suitable candidates for applications such as gas storage,[1,2] gas separation,[3,4] catalysis,[5,6] luminescence,[7,8] optoelectronics,[9,10] and drug delivery.[11,12] Because their mechanical stability is crucial for any technological application,[13] understanding their mechanical behavior assumes singular importance. Though there have been a few recent studies of linear elastic response of these framework materials to mechanical stress,[14,15] their response beyond the elastic limit has not been adequately explored.

ZIF-8 ($Zn(mIm)_2$, mIm = 2-methylimidazolate) with the sodalite (SOD) topology, crystallizes in the cubic space group $I\bar{4}3m$ (Figure 1a) with a lattice constant of 16.992 Å,[16] and contains 276 atoms in the unit cell ($Zn_{12}N_{48}C_{96}H_{120}$). It exhibits an exceptionally large pore volume, with a solvent-accessible volume (SAV) of ∼50%.[17] Recently, Tan et al.[14] studied the complete *linear* elastic response of ZIF-8 and reported an exceptionally low shear modulus of 0.97 GPa. This result suggested easy mechanical failure of ZIF-8 upon the application of shear stresses, which was later confirmed by Cao et al.[18] who reported its rapid amorphization upon ball milling. This work explores the *nonlinear* shear and cleavage response of ZIF-8 to identify a possible mechanism of its amorphization during ball milling.

We study the nonlinear response of ZIF-8 with respect to two crystallographic modes of failure, cleavage and shear. The former occurs as a result of tensile stresses acting normal to a crystallographic cleavage plane, for which the energy rate necessary is twice the surface energy, as per the Griffith criterion.[19] The latter occurs under the influence of shear stresses, resulting in extensive slip of dislocations and the formation of stacking faults, the energetics of which are captured in the generalized stacking fault energy (GSF) surface or the γ-surface.[20]

We have used a combination of two first-principles methods in our investigation, (a) density functional theory (DFT) as implemented in the Vienna ab initio simulation package (VASP)[21] and (b) the density functional tight binding (DFTB) method as implemented in DFTB+.[22] In the DFT-based calculations, ion−electron interactions were modeled using ultrasoft pseudopotentials,[23] and the exchange−correlation functional was approximated by the generalized gradient approximation (GGA) as parametrized by Perdew and Wang (1991).[24] Because the DFT-based calculations were computationally very expensive, DFTB-based calculations were used for simulating the system on a larger scale. Slater−Koster files from the parameter set *znorg-0-1*[25] were used to parametrize the interactions between the elements in the system. DFTB has been successfully used to calculate the structural properties of MOFs previously,[26] and we further benchmarked its parameters through comparison of its results for the stacking fault energy (SFE) with those by DFT (within 5%). van der Waals (vdW)

Received: August 6, 2013
Accepted: September 22, 2013
Published: September 23, 2013

   dx.doi.org/10.1021/jz4016734 | *J. Phys. Chem. Lett.* 2013, 4, 3377−3381

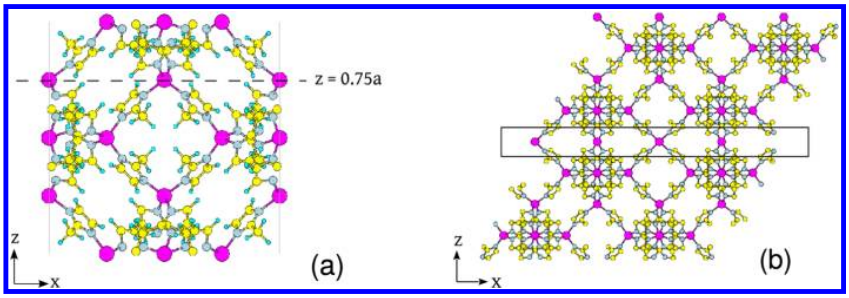

Figure 1. (a) Unit cell of ZIF-8; (b) ISF structure with a slip vector $(x,y) = (0.50,0.50)$, with one SF per unit cell. The stacking fault has been enclosed by a box. It has two unit cells each in the x, y, and z directions for better visualization. Zinc atoms are shown in pink, nitrogen atoms in blue, carbon atoms in yellow, and hydrogen atoms in cyan. Hydrogen atoms have been omitted for clarity in (b).

interactions were included with a Lennard-Jones dispersion model as in DFTB+,[27] with parameters for the potential taken from the Universal Force Field (UFF).[28] We checked the convergence of total energy with respect to the fineness of the k mesh used and observed that a $1 \times 1 \times 1$ mesh was sufficiently accurate (within 0.1 meV/unit cell) for our calculations. The positions of the atoms in a unit cell were relaxed, keeping the lattice constant fixed at the experimental value, by minimizing the energy until Hellman−Feynman forces were within 0.002 Ry/Å. The Hessian matrix was evaluated numerically using a method of finite differences with a symmetric finite differences formula on Hellman−Feynman forces and atomic displacements of ±0.01 Å.

We focus on stacking faults generated on the (001) plane in ZIF-8, with a transformation of the unit cell vector

$$\vec{c} = \vec{c}_o + x\vec{a} + y\vec{b} \tag{1}$$

where $\vec{a}$, $\vec{b}$, and $\vec{c}$ are the unit cell vectors. The corresponding SFEs were obtained by calculating the difference between the energy of the faulted and ideal structures. The energy as a function of x and y defines the γ-surface, $Z = E(x,y)$. Due to the complexity of the hierarchical structure, not all (001) planes in ZIF-8 are equivalent, in contrast to simple metals whose crystal structures have only one or two atoms per unit cell. We chose the z-plane across which the fewest number of bonds are affected by a stacking fault, that is, at $z = 0.75a$.

We used a uniform 4×4 mesh in the real space planar (the (001) plane) unit cell to interpolate the data to construct a γ-surface. We have checked the numerical values obtained from the interpolation formula for the underlying symmetry and sufficient accuracy. Specifically, we used the following expression

$$\gamma(x, y) = 0.2 \sum_{m=1}^{5} \sum_{n=1}^{5} A_{m,n} \exp\{i(2\pi k_m x + 2\pi k_n y)\} \tag{2}$$

where $k = \{0,1,2,-2,-1\}$ and $A_{m,n}$ are coefficients obtained from a discrete Fourier transform of the stacking fault energies ($SFE_{m,n}$) calculated on the 4×4 spatial mesh. The coefficients $A_{m,n}$ bear the symmetry of the crystal.

The energy relevant to the tensile mode of failure is the surface energy (γ_s), which is defined as the difference between the total energy of the bulk and that of the crystal cleaved across the required plane (here, (001) with $z = 0.75a$). Our estimate of γ_s for ZIF-8 is ∼280 mJ/m^2, around 5−6 times lower than that of soft, ductile metals like copper (∼1.73 J/m^2) and gold (∼1.48 J/m^2),[29] both of which are cubic close-packed, and that of covalently bonded solids like Si (∼1.36 J/m^2),[30] which has diamond cubic structure.

A γ-surface is generated through interpolation of energies in Table 1 according to eq 2. A minimum of the γ-surface represents the intrinsic SFE (γ_{isf}) of a material. For ZIF-8, it occurs at a shift (Figure 2) of $(0.50,0.50)a$ (the structure with the corresponding SF is referred to henceforth as the ISF structure) with a surprisingly low γ_{isf} (∼66 mJ/m^2) comparable to that of metals like copper and gold[31] and covalently bonded Si.[30] This implies that the stacking faults in ZIF-8, if present, should be wide and visible through transmission electron microscopy. In practice though, the templating effect by the solvent molecules may hinder the formation of such faults, and they may not occur as commonly as expected from the energetics. A possible dissociation reaction of the dislocation with Burgers vector $a_o\langle 110\rangle$, on the (001) plane, is

$$a_o\langle 110\rangle = \frac{a_o}{2}\langle 110\rangle + \mathrm{SF} + \frac{a_o}{2}\langle 110\rangle$$

which results in two collinear partials and an intrinsic stacking fault.

The unstable stacking energy (γ_{usf}) of a material is defined as the lowest-energy barrier to be crossed to go from the ideal structure to the ISF structure. For ZIF-8, the barrier occurs at a shift of $(0.25,0.25)a$ (the structure with the corresponding SF is referred to henceforth as the USF structure) with an estimated energy of ∼434 mJ/m^2. This is around 3−4 higher than that of metals like copper and gold[29] and around 4−5 times lower than that of covalently bonded materials like Si.[30] The ratio of surface energy to unstable SFE characterizes the brittle versus ductile tendency of a material and is termed the disembrittlement parameter ($D = \gamma_s/\gamma_{usf}$).[32] On this basis, our estimate of D for ZIF-8 is 0.64, which means that it is brittle, that is, it is easier to cleave than to nucleate a dislocation necessary for plastic deformation. This preferential brittle failure may also prevent the stacking faults from occurring in ZIF-8, despite the

Table 1. Stacking Fault Energies Obtained from DFT-Based Calculations

x	y	fault energy (mJ/m^2)
0.00	0.00	0.0
0.25	0.00	479.5
0.25	0.25	434.1
0.50	0.00	491.7
0.50	0.25	458.1
0.50	0.50	65.9

dx.doi.org/10.1021/jz4016734 | J. Phys. Chem. Lett. 2013, 4, 3377−3381

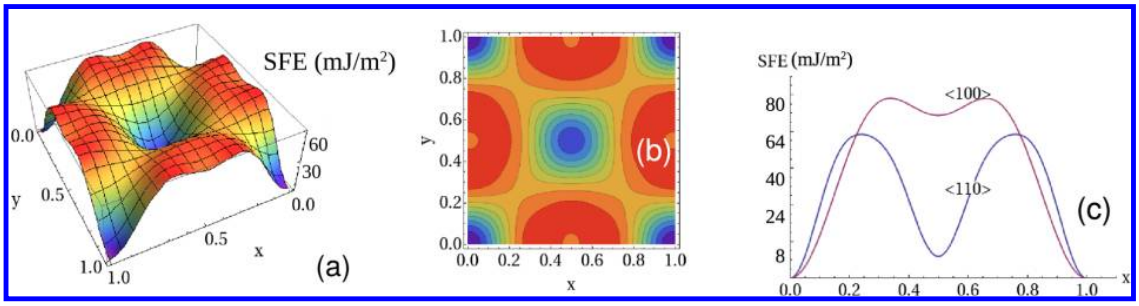

Figure 2. (a) The γ-surface for the {100} plane in ZIF-8. (b) Contour plot of the γ-surface for the {100} plane in ZIF-8. (c) Sections of the γ-surface along ⟨100⟩ and ⟨110⟩.

low γ_{isf}. This result is consistent with experimental observations in which the single crystals of hybrid frameworks are indeed susceptible to material failure by cracking and thereby exhibit a low fracture toughness.[13]

To further verify the reliability of our findings, we calculated the energies of lower density stacking faults (i.e., one stacking fault per two unit cells) (Table 2). It can be seen that the energy cost of introducing a stacking fault per two unit cells is within 4% of that for one fault per unit cell, which leads us to conclude that interaction between stacking faults in ZIF-8 is weak. This result also suggests that the properties of the stacking faults are essentially dependent only on the local framework structure. Interestingly, inclusion or exclusion of vdW interactions using DFTB (Table 2) yielded no notable changes in the SFEs.

Table 2. Comparison of SFE Calculated Using DFT, DFTB, and DFTB+vdW Based Calculations For 1 SF Per Unit Cell and 1 SF Per 2 Unit Cells

method	1 SF/unit cell fault energy (mJ/m^2)	1 SF/2 unit cells fault energy (mJ/m^2)
DFT	65.87	63.43
DFTB	69.42	67.87
DFTB +vdW	70.92	67.92

The relaxed ISF structure (Figure 1b) reveals that the local atomic structure does not change upon introduction of SFs, and this conservation of local order suggests a low SFE, which is indeed consistent with our calculations in Table 1. We note that only Zn−N bonds are affected by shear or cleavage across the (001) plane at $z = 0.75a$, and these get re-formed in the ISF configuration. A comparison of the electronic density of states (DoS) for the ideal and ISF structures (Figure 3a) reveals no conspicuous differences, particularly across the gap. By projecting the total density of electronic states onto atomic orbitals, we find that (i) the valence band is composed almost entirely of C-2p orbitals while Zn-3d states are deep lying in energy (~4.5 eV lower than the valence band maximum), (ii) the conduction band has equal contributions from C-2p and N-2p orbitals, and (iii) these remain unaffected upon the introduction of SFs. Because valence and conduction states interact effectively with a guest moiety, it is expected that gas adsorption, catalysis, and other related properties of ZIF-8 will remain largely unaffected by stacking faults.

The Hessian of the total energy obtained from DFTB calculations was used to determine vibrational frequencies and modes of ZIF-8. A comparison of the vibrational DoS of the ideal and ISF structures (Figure 3b) shows the splitting of a group of modes at ~1280 cm^{-1} into two separate groups of modes at ~1260 and ~1230 cm^{-1}, which should constitute a Raman signature of the SFs. These modes correspond to stretching of the imidazolate ring along the Zn−Im−Zn axis or perpendicular to it. Upon the introduction of a fault, the imidazolate rings away from the fault participate in the modes at ~1260 cm^{-1}, while those closest to the fault participate in the modes at ~1230 cm^{-1}, indicating that chemical bonds in the imidazolate rings near the fault weaken.

Although such faults have been observed in covalent−organic frameworks (COFs),[33] they are yet to be reported in ZIFs, suggesting that such faults may not be common in ZIF-8 and that alternative structures that may be more favorable to the ones with faults may exist. To this end, we determined the vibrational spectrum of the state corresponding to the energy barrier (USF structure) that ZIF-8 must pass through to develop a fault, to analyze its local structural stability. An

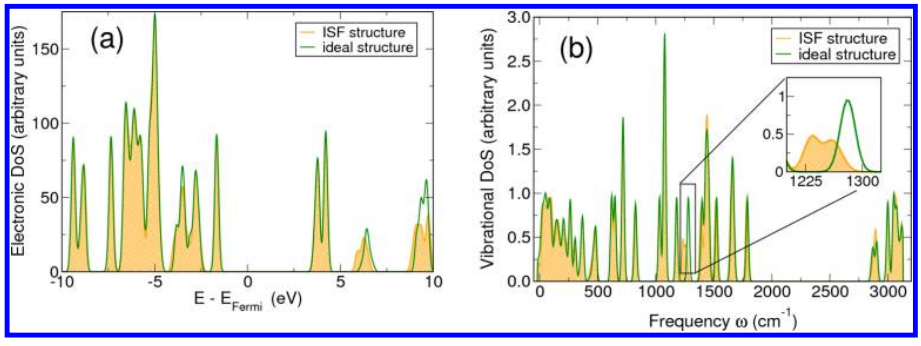

Figure 3. Comparison of (a) vibrational and (b) electronic DoS for the ideal and ISF structures.

dx.doi.org/10.1021/jz4016734 | J. Phys. Chem. Lett. 2013, 4, 3377−3381

inspection of the vibrational DoS of the USF structure reveals structural instabilities through imaginary frequencies (Figure 4).

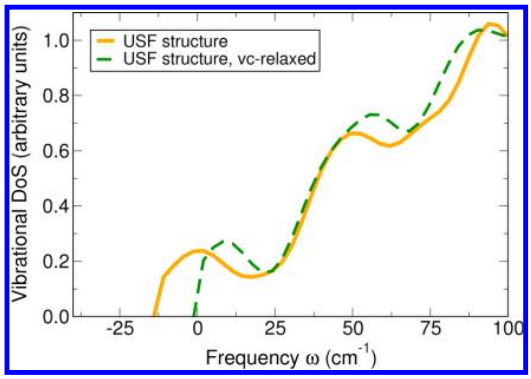

Figure 4. Comparison of the vibrational DoS of the USF structure, before and after variable-cell optimization (vc-relaxed), revealing local instabilities.

Second, the USF state also exhibits a compressive stress. The presence of a compressive stress state on the structure prompted us to perform variable-cell (complete) relaxation, which resulted in a reduction of the cell volume by ∼10% (or a corresponding increase in the density by ∼11%). We expect similar structural instabilities of the USF structures arising during slips on other symmetry-equivalent planes of the {100} family, that is, the (100) and (010) planes (along with those on the (001) plane studied here), to lead to further reduction in the cell volume (or correspondingly, a further increase in the density). As seen earlier, the energy barriers during slip to the faulted structure are quite high. Because there is no high-density crystalline phase ZIF-zni associated with ZIF-8,[34] the structural instabilities and the associated compressive stress state transform the barrier (transition) state into a lower-energy disordered structure of higher density, providing an alternate pathway to the amorphous phase aZIF-8. In this connection, we note that a recent calorimetric study has shown that the amorphous state is only 4.5 kJ mol^{-1} less stable than the denser phase for ZIFs containing unsubstituted imidazole ligands.[35]

We have studied the nonlinear mechanical behavior of a prototypical imidazole-based MOF, ZIF-8, by simulating uniaxial tensile and shear modes of failure. We expect ZIF-8 to be intrinsically brittle because it is easier to cleave than to nucleate a dislocation to enable plastic flow. A very low intrinsic SFE, comparable to copper and gold, leads us to expect the SFs in ZIF-8 to be wide, if present. We identify a Raman signature of the SFs, characterized by the splitting of a peak at ∼1280 cm^{-1} into two distinct peaks at ∼1260 and ∼1230 cm^{-1}. We find that stacking faults do *not* alter the local atomic structure or the electronic structure of ZIF-8 and therefore are not detrimental to its physicochemical properties, auguring well for its practical applications. The lack of evidence for such faults in experiments is explained through the preferential formation of the high-density amorphous phase through the release of shear and compressive stresses acting on the USF state present as a barrier.

AUTHOR INFORMATION

Corresponding Authors

*E-mail: waghmare@jncasr.ac.in (U.V.W.).
*E-mail: akc30@cam.ac.uk (A.K.C.).

Notes

The authors declare no competing financial interest.

ACKNOWLEDGMENTS

The authors acknowledge the Centre for Computational Materials Science (CCMS), Jawaharlal Nehru Centre for Advanced Scientific Research (JNCASR) for providing access to computational facilities used to perform some of the calculations in this work. J.-C.T. and A.K.C. thank the European Research Council for providing financial support.

REFERENCES

(1) Morris, R.; Wheatley, P. Gas Storage in Nanoporous Materials. *Angew. Chem., Int. Ed.* **2008**, *47*, 4966−4981.
(2) Farha, O. K.; Yazaydin, A. Ö.; Eryazici, I.; Malliakas, C. D.; Hauser, B. G.; Kanatzidis, M. G.; Nguyen, S. T.; Snurr, R. Q.; Hupp, J. T. *De novo* Synthesis of a Metal−Organic Framework Material Featuring Ultrahigh Surface Area and Gas Storage Capacities. *Nat. Chem.* **2010**, *2*, 944−948.
(3) Li, J.-R.; Kuppler, R. J.; Zhou, H.-C. Selective Gas Adsorption and Separation in Metal−Organic Frameworks. *Chem. Soc. Rev.* **2009**, *38*, 1477−1504.
(4) Chen, B.; Liang, C.; Yang, J.; Contreras, D. S.; Clancy, Y. L.; Lobkovsky, E. B.; Yaghi, O. M.; Dai, S. A Microporous Metal−Organic Framework for Gas-Chromatographic Separation of Alkanes. *Angew. Chem., Int. Ed.* **2006**, *45*, 1390−1393.
(5) Lee, J.; Farha, O. K.; Roberts, J.; Scheidt, K. A.; Nguyen, S. T.; Hupp, J. T. Metal−Organic Framework Materials as Catalysts. *Chem. Soc. Rev.* **2009**, *38*, 1450−1459.
(6) Ma, L.; Abney, C.; Lin, W. Enantioselective Catalysis with Homochiral Metal−Organic Frameworks. *Chem. Soc. Rev.* **2009**, *38*, 1248−1256.
(7) Allendorf, M. D.; Bauer, C. A.; Bhakta, R. K.; Houk, R. J. T. Luminescent Metal−Organic Frameworks. *Chem. Soc. Rev.* **2009**, *38*, 1330−1352.
(8) Chen, B.; Wang, L.; Zapata, F.; Qian, G.; Lobkovsky, E. B. A Luminescent Microporous Metal−Organic Framework for the Recognition and Sensing of Anions. *J. Am. Chem. Soc.* **2008**, *130*, 6718−6719.
(9) Evans, O. R.; Lin, W. Crystal Engineering of NLO Materials Based on Metal−Organic Coordination Networks. *Acc. Chem. Res.* **2002**, *35*, 511−522.
(10) Lin, W.; Wang, Z.; Ma, L. A Novel Octupolar Metal−Organic NLO Material Based on a 2D Coordination Network. *J. Am. Chem. Soc.* **1999**, *121*, 11249−11250.
(11) Horcajada, P.; et al. Porous Metal−Organic Framework Nanoscale Carriers as a Potential Platform for Drug Delivery and Imaging. *Nat. Mater.* **2010**, *9*, 172−178.
(12) Vallet-Regí, M.; Balas, F.; Arcos, D. Mesoporous Materials for Drug Delivery. *Angew. Chem., Int. Ed.* **2007**, *46*, 7548−7558.
(13) Tan, J. C.; Cheetham, A. K. Mechanical Properties of Hybrid Inorganic−Organic Framework Materials: Establishing Fundamental Structure−Property Relationships. *Chem. Soc. Rev.* **2011**, *40*, 1059−1080.
(14) Tan, J.-C.; Civalleri, B.; Lin, C.-C.; Valenzano, L.; Galvelis, R.; Chen, P.-F.; Bennett, T. D.; Mellot-Draznieks, C.; Zicovich-Wilson, C. M.; Cheetham, A. K. Exceptionally Low Shear Modulus in a Prototypical Imidazole-Based Metal−Organic Framework. *Phys. Rev. Lett.* **2012**, *108*, 095502.
(15) Ortiz, A. U.; Boutin, A.; Fuchs, A. H.; Coudert, F. m. c.-X. Anisotropic Elastic Properties of Flexible Metal−Organic Frameworks: How Soft are Soft Porous Crystals? *Phys. Rev. Lett.* **2012**, *109*, 195502.
(16) Moggach, S.; Bennett, T.; Cheetham, A. The Effect of Pressure on ZIF-8: Increasing Pore Size with Pressure and the Formation of a High-Pressure Phase at 1.47 GPa. *Angew. Chem., Int. Ed.* **2009**, *48*, 7087−7089.
(17) Tan, J. C.; Bennett, T. D.; Cheetham, A. K. Chemical Structure, Network Topology, and Porosity Effects on the Mechanical Properties

of Zeolitic Imidazolate Frameworks. *Proc. Natl. Acad. Sci. U.S.A.* **2010**, *107*, 9938−9943.
(18) Cao, S.; Bennett, T. D.; Keen, D. A.; Goodwin, A. L.; Cheetham, A. K. Amorphization of the Prototypical Zeolitic Imidazolate Framework ZIF-8 by Ball-Milling. *Chem. Commun.* **2012**, *48*, 7805−7807.
(19) Griffith, A. A. The Phenomena of Rupture and Flow in Solids. *Philos. Trans. R. Soc. London, Ser. A* **1921**, *221*, 163−198.
(20) Vitek, V. Intrinsic Stacking Faults in Body-Centred Cubic Crystals. *Philos. Mag.* **1968**, *18*, 773−786.
(21) Kresse, G.; Furthmüller, J. Efficiency of Ab-Initio Total Energy Calculations for Metals and Semiconductors Using a Plane-Wave Basis Set. *Comput. Mater. Sci.* **1996**, *6*, 15−50.
(22) Aradi, B.; Hourahine, B.; Frauenheim, T. DFTB+, a Sparse Matrix-Based Implementation of the DFTB Method. *J. Phys. Chem. A* **2007**, *111*, 5678−5684.
(23) Vanderbilt, D. Soft Self-Consistent Pseudopotentials in a Generalized Eigenvalue Formalism. *Phys. Rev. B* **1990**, *41*, 7892−7895.
(24) Perdew, J. P.; Wang, Y. Accurate and Simple Analytic Representation of the Electron−Gas Correlation Energy. *Phys. Rev. B* **1992**, *45*, 13244−13249.
(25) Moreira, N. H.; Dolgonos, G.; Aradi, B.; da Rosa, A. L.; Frauenheim, T. Toward an Accurate Density-Functional Tight-Binding Description of Zinc-Containing Compounds. *J. Chem. Theory Comput.* **2009**, *5*, 605−614.
(26) Lukose, B.; Supronowicz, B.; Petkov, P. S.; Frenzel, J.; Kuc, A. B.; Seifert, G.; Vayssilov, G. N.; Heine, T. Structural Properties of Metal−Organic Frameworks within the Density-Functional Based Tight-Binding Method. *Phys. Status Solidi B* **2012**, *249*, 335−342.
(27) Elstner, M.; Hobza, P.; Frauenheim, T.; Suhai, S.; Kaxiras, E. Hydrogen Bonding and Stacking Interactions of Nucleic Acid Base Pairs: A Density-Functional-Theory Based Treatment. *J. Chem. Phys.* **2001**, *114*, 5149−5155.
(28) Rappe, A. K.; Casewit, C. J.; Colwell, K. S.; Goddard, W. A.; Skiff, W. M. UFF, a Full Periodic Table Force Field for Molecular Mechanics and Molecular Dynamics Simulations. *J. Am. Chem. Soc.* **1992**, *114*, 10024−10035.
(29) Mehl, M. J.; Papaconstantopoulos, D. A.; Kioussis, N.; Herbranson, M. Tight-Binding Study of Stacking Fault Energies and the Rice Criterion of Ductility in the FCC Metals. *Phys. Rev. B* **2000**, *61*, 4894−4897.
(30) Eaglesham, D. J.; White, A. E.; Feldman, L. C.; Moriya, N.; Jacobson, D. C. Equilibrium Shape of Si. *Phys. Rev. Lett.* **1993**, *70*, 1643−1646.
(31) Dieter, G. E. *Mechanical Metallurgy*; McGraw-Hill Book Company: London, 1988.
(32) Waghmare, U. V.; Kaxiras, E.; Bulatov, V. V.; Duesbery, M. S. Effects of Alloying on the Ductility of $MoSi_2$ Single Crystals from First-Principles Calculations. *Modell. Simul. Mater. Sci. Eng.* **1998**, *6*, 493−506.
(33) Côté, A. P.; Benin, A. I.; Ockwig, N. W.; O'Keeffe, M.; Matzger, A. J.; Yaghi, O. M. Porous, Crystalline, Covalent Organic Frameworks. *Science* **2005**, *310*, 1166−1170.
(34) Bennett, T. D.; Goodwin, A. L.; Dove, M. T.; Keen, D. A.; Tucker, M. G.; Barney, E. R.; Soper, A. K.; Bithell, E. G.; Tan, J.-C.; Cheetham, A. K. Structure and Properties of an Amorphous Metal−Organic Framework. *Phys. Rev. Lett.* **2010**, *104*, 115503.
(35) Hughes, J. T.; Bennett, T. D.; Cheetham, A. K.; Navrotsky, A. Thermochemistry of Zeolitic Imidazolate Frameworks of Varying Porosity. *J. Am. Chem. Soc.* **2013**, *135*, 598−601.